arXiv:1610.02197v1 [nucl-th] 7 Oct 2016



New exact solutions of hydrodynamics for rehadronizing fireballs with lattice QCD equation of state

T. Csörgő[1,2] and G. Kasza[3],

[1]Wigner RCP, H - 1525 Budapest 114, P.O.Box 49, Hungary,
[2]EKU KRC, H-3200 Gyöngyös, Mátrai út 36, Hungary,
[3]Eötvös Loránd University, H-1117 Budapest, Pázmány P. s. 1/A, Hungary

March 5, 2024

Abstract

We describe fireballs that rehadronize from a perfectly fluid quark matter to a chemically frozen, multi-component hadron gas. In the hydrodynamics of these fireballs, we utilize the lattice QCD equation of state, however, we also apply non-relativistic kinematics for simplicity and clarity. Two new classes of exact, analytic solutions of fireball hydrodynamics are presented: the first class describes triaxially expanding, non-rotating ellipsoidal fireballs, while the second class of exact solutions corresponds to spheroidally symmetric, rotating fireballs. In both classes of solutions, we find evidence for a secondary explosion, that happens just after hadrochemical freeze-out. A realistic, linear mass scaling of the slope parameters of the single particle spectra of various hadronic species is obtained analytically, as well as an also realistic, linear mass scaling of the inverse of the squared HBT radius parameters of the Bose-Einstein correlation functions.

1 Introduction

The equations of hydrodynamics contain no internal scale, and the applications of hydrodynamics range from the largest, cosmological distances to the smallest experimentally accessible distances. Hydrodynamical type of equations characterize the time evolution of our Universe that started from a Big Bang. Hydrodynamics is also applied to the study of the time evolution on the smallest, femtometer distances, where the Little Bangs of high energy heavy ion collisions also create hydrodynamically evolving fireballs. Our Universe about 14 billion years after the Big Bang expands with an approximately spherically symmetric Hubble flow. The hadronic final states of heavy ion collisions about a few times 10^{-23} sec after the Little Bangs expand with directional Hubble flows and possibly also with significant angular momentum, due to the typically non-central nature of high energy heavy ion collisions.

As early as in 1978, Zimányi, Bondorf and Garpman found an exact solution of hydrodynamics that described a non-relativistic, finite fireball with a Hubble flow, expanding to vacuum [1]. Keeping the spherical symmetry and the Hubble flow profile, the Zimányi-Bondorf-Garpman solution was generalized in 1998, after 20 years, to a spatially Gaussian density and a spatially homogeneous temperature profile, while maintaining the same equations for the time evolution of the scales as in the Zimányi-Bondorf-Garpman solution [2]. Soon it was realized that these solutions can be generalized to arbitrary, but matching temperature and density profile functions, while still maintaining spherical [3] symmetry. Within a few years, the first, spherically symmetric solutions were successfully generalized to include ellipsoidal symmetries [4, 5]. About at the same time, the Gaussian solutions were utilized to evaluate the final state hadronic observables and their relation to the initial conditions, as it turned out that these solutions provided exact results for the single particle spectra, elliptic and higher order flows, as well as for the Bose-Einstein correlation functions [6]. In this class of solutions, a non-vanishing initial angular momentum and the corresponding rotation of the expanding fireball can also be taken into account analytically. The first exact solution of rotating fireball hydrodynamics was found in the relativistic kinematic region [7]. This spheroidally symmetric, relativistic rotating solution was subsequently generalized to the non-relativistic kinematic domain [8, 9, 10], including not only spheroidally but also triaxially expanding and rotating solutions of fireball hydrodynamics. In these solutions, the hadronic final state was typically containing only a given type of particle with mass m, and the observables like the slope parameters of the single particle spectra were investigated as a function of this mass, considered to be a parameter of the solution.

This conference presentation details the first steps towards generalizing some of the

recently found expanding as well as rotating, spheroidally and ellipsoidally symmetric solutions of fireball hydrodynamics [8, 9, 10] to a more realistic hadro-chemical and kinetic freeze-out stage. These final states contain a mixture of hadrons, with different hadronic masses denoted as m_i. In this work, we explore two classes of exact solutions. The first class describes triaxially expanding, non-rotating ellipsoidal fireballs, the second class of exact solutions corresponds to spheroidally symmetric, rotating fireballs. In both classes of exact solutions, lattice QCD calculations provide the data for the equations of state. This allows us to take into account the temperature dependence of the speed of sound, following refs. [6, 11]. After rehadronization, a subsequent hadrochemical freeze-out is shown to have a significant effect on the expansion dynamics, corresponding to a secondary explosion, which is seen in in both classes of exact solutions. The properties and the criteria of such a secondary explosion are clarified here in an exact and analytic manner.

2 Perfect fluid hydrodynamics for two different stages

Experimental results of the NA44 [12] as well as the PHENIX collaborations [13] indicate, for example, that the so called inverse slope parameter of the single particle spectra is a linear function of the mass m of the observed hadrons:

$$T = T_f + m\langle u_t\rangle^2, \tag{1}$$

where $\langle u_t\rangle$ stands for the average radial flow and the freeze-out temperature is denoted by T_f. This relationship has been derived even for non-central heavy ion collisions in ref. [6], taking into account a chemically frozen, *single component* hadronic matter (HM). However, the experimental data were taken in heavy ion collisions where actually several different kind of hadrons are produced simultaneously. If we introduce an index "i" to distinguish the different particle types in a multi-component hadron gas, then the experimental data indicate that the slope parameters depend on the particle type only through the mass m_i of particle type i, but the radial flow $\langle u_t\rangle$ and the kinetic freeze-out temperature T_f are both independent of the type of the particles:

$$T_i = T_f + m_i\langle u_t\rangle^2. \tag{2}$$

In this work, we analytically derive these relations, for a fireball of a strongly interacting Quark Gluon Plasma that hadronizes to a *multi-component,* chemically frozen hadronic matter or HM.

The basic equations of perfect fluid hydrodynamics are given by the continuity and the Euler equation together with the energy equation, corresponding to local conservation of entropy, momentum and energy. In the strongly coupled Quark-Gluon Plasma, also called

as perfect fluid of Quark Matter or QM, and at vanishing baryochemical potential, the number of quarks, anti-quarks and gluons is not conserved individually, only the local conservation of entropy drives the expansion. However, at a certain temperature various hadrons are produced due to rehadronization from a QM and we assume in this manuscript that the inelastic reactions that may transform one hadron to another are negligible, so we study here the scenario that corresponds to a chemically frozen, multi-component Hadronic Matter (HM). In this chemically frozen, multi-component HM phase the number of each type of hadrons is locally conserved.

The equations of motion for these two different forms of matter are summarized in Table 1. These equations generalize the equations of motion for a chemically frozen, *single component* hadronic matter equations of (13-16) of ref. [8] to the case of the chemically frozen, *multi-component* scenario of HM. The local momentum and energy conservation, as well as the entropy conservation is valid in both phases, but in the HM phase, local continuity equations are also obeyed for all hadronic species. We utilize the $\epsilon = \kappa p$ equation of state (EoS), where $\kappa \equiv \kappa(T)$ is a temperature dependent function, that is directly taken from lattice QCD calculations of ref. [14]. We note that in Table 1 the energy equations are rewritten for the temperature field. We also note that due to the additional local conservation laws in the HM phase the coefficient of the co-moving time derivative of the temperature field changes in the temperature equation in Table 1. It turnes out that this leads to a dynamical effect, a modification for the time evolution of the temperature. This modification corresponds to a secondary explosion that starts at the chemical freeze-out temperature T_{chem}.

In Table 1, $\sigma \equiv \sigma(\mathbf{r}, t)$ stands for the entropy density, $n_i \equiv n_i(\mathbf{r}, t)$ is the density of hadron type i that is locally conserved in the HM phase, the velocity field is denoted by $\mathbf{v} \equiv \mathbf{v}(\mathbf{r}, t)$, while $p \equiv p(\mathbf{r}, t)$ stands for the pressure, and $T \equiv T(\mathbf{r}, t)$ for the temperature field, and the mass of hadron type i is denoted as m_i.

As discussed in ref. [8], these equations were derived in the non-relativistic limit of the equations of relativistic hydrodynamics, assuming that the entalphy density (that characterizes the inertia of the motion for pressure gradients) is dominated by the entropy density above the chemical freeze-out temperature, while it is dominated by the mass terms of the hadrons at lower temperatures:

$$\varepsilon + p = \sum_i \mu_i n_i + T\sigma, \tag{3}$$

$$\varepsilon + p \approx T\sigma, \qquad (T_i \geq T \geq T_{chem}), \tag{4}$$

$$\varepsilon + p \approx \sum_i m_i n_i \qquad (T_{chem} > T \geq T_f). \tag{5}$$

The dynamical equations, summarized in Table 1, can be solved if the usual initial and

QM ($T_i \geq T \geq T_{chem}$)	**HM** ($T_{chem} > T \geq T_f$)
$\partial_t \sigma + \nabla (\sigma \mathbf{v}) = 0$	$\partial_t n_i + \nabla (n_i \mathbf{v}) = 0, \quad \forall i$
$T\sigma (\partial_t + \mathbf{v}\nabla) \mathbf{v} = -\nabla p$	$\sum_i m_i n_i (\partial_t + \mathbf{v}\nabla) \mathbf{v} = -\nabla p$
$\frac{1+\kappa}{T} \left[\frac{d}{dT} \frac{\kappa T}{1+\kappa} \right] (\partial_t + \mathbf{v}\nabla) T + \nabla \mathbf{v} = 0$	$\frac{1}{T} \left[\frac{d(\kappa T)}{dT} \right] (\partial_t + \mathbf{v}\nabla) T + \nabla \mathbf{v} = 0$
$p = \sigma T/(1+\kappa)$	$p = \sum_i p_i = T \sum_i n_i$

Table 1: Hydrodynamical equations for strongly interacting Quark Gluon Plasma or Quark Matter (QM) and chemically frozen, multi-component Hadronic Matter (HM) that drive the fireball expansion from the initial temperature T_i to the chemical freeze-out temperature ($T_i \geq T \geq T_{chem}$). This chemical freeze-out temperature T_{chem} characterizes both hadronization and simultaneous hadrochemical freeze-out in the present manuscript. Below this chemical freeze-out temperature but above the kinetic freeze-out temperature ($T_{chem} > T \geq T_f$), a multi-component hadronic matter is characterized by local conservation laws for each hadronic species.

freeze-out conditions as well as the chemical freeze-out conditions are given. In the present work, we characterize these conditions by the initial temperature T_i, the chemical freeze-out temperature T_{chem} and by the kinetic freeze-out temperature T_f.

In this manuscript, we also assume that the initial temperature distribution is locally homogeneous, and its value is given by a coordinate independent T_i value at the initial time $t_i = 0$, and we also assume that the HM freezes out at a locally homogeneous freeze-out temperature T_f. In addition to these usual initial and final boundary conditions, in these solutions we also have to specify a matching boundary conditions that specifies the transition from QM to HM, which we characterize by the locally homogeneous chemical freeze-out temperature T_{chem}.

We suppose that rehadronization happens almost simultaneously with the hadrochemical freeze-out at the time $t = t_c$, and at this temperature the local velocity fields transfer smoothly:

$$T_B(t_c) = T_A(t_c) = T_{chem}, \tag{6}$$

$$\mathbf{v}_B(t_c, \mathbf{r}) = \mathbf{v}_A(t_c, \mathbf{r}). \tag{7}$$

The medium before the rehadronization is in the QM phase, its parameters are indicated by B that stands for Before. After the rehadronization, we use the A index, it indexes the medium that is converted to the HM phase. We follow Landau's proposal, who suggested

that at the time of rehadronization a conversion takes place between entropy density and particle density [15]. Therefore we assume that

$$\frac{\sigma(\mathbf{r}, t_c)}{\sigma(\mathbf{r}=0, t_c)} = \frac{n_i(\mathbf{r}, t)}{n_i(\mathbf{r}=0, t_c)}. \tag{8}$$

We look for parametric solutions of the hydrodynamical equations, summarized in Table 1, and we assume that the principal axes of a triaxially expanding, ellipsoidal fireball are be given by $X \equiv X(t)$, $Y \equiv Y(t)$ and $Z \equiv Z(t)$ that functions depend only on the time t.

In this manuscript, we discuss two classes of parametric, exact solutions of fireball hydrodynamics. The first class is a triaxial, non-rotating class of solutions, while the second class corresponds to a spheroidally symmetric, rotating class of exact solutions of fireball hydrodynamics. In the triaxial case, all the principal axis (X, Y, Z) can be different, but the initial angular velocity ω_0 has to vanish. For the rotating solutions of fireball hydrodynamics with non-vanishing initial angular velocity, we assume spheroidal symmmetry and introduce the notation $X(t) = Y(t) = R(t)$.

All of the scale functions (X, Y, Z) as well as R are continuous at t_c, and it turns out that we can follow the lines of derivations described in refs. [5, 8, 9] even for an QM that rehadronizes to a HM, without introducing a particle species dependence of the scale parameters (X, Y, Z) after the rehadronization. The details of these calculations are not given here, but the main results are summarized in Table 2 for a tri-axially expanding, non-rotating ellipsoidal fireball, and Table 3 for a spheroidal, rotating and expanding fireball. These results indicate that the rather complicated partial differential equations that govern the dynamics of the fireball expansion can be solved exactly, when the hydrodynamical fields are given in terms of the scale parameters of the solutions. Thus these solutions are parametric solutions, the scale parameters (X, Y, Z) satisfy a system of coupled and non-linear but ordinary differential equations, listed also in Tables 2 and 3. These differential equations can be readily solved with currently available numerical packages like MATHEMATICA or MATLAB .

For a triaxially expanding ellipsoid, the volume of the fireball is given by that of a 3d Gaussian with widths X, Y and Z:

$$V(t) = (2\pi)^{3/2} XYZ, \tag{9}$$

while for a spheroidally expanding ellipsoid, $X = Y = R$ and the volume is given by

$$V(t) = (2\pi)^{3/2} R^2 Z. \tag{10}$$

In the considered class of exact, rotating spheroidal solution the angular velocity is driven

QM ($T_i \geq T \geq T_{chem}$)	**HM** ($T_{chem} > T \geq T_f$)
$\mathbf{v} = (\frac{\dot{X}}{X} r_x, \frac{\dot{Y}}{Y} r_y, \frac{\dot{Z}}{Z} r_z)$	$\mathbf{v} = (\frac{\dot{X}}{X} r_x, \frac{\dot{Y}}{Y} r_y, \frac{\dot{Z}}{Z} r_z)$
$\sigma = \sigma_0 \frac{V_0}{V} \exp\left(-\frac{r_x^2}{2X^2} - \frac{r_y^2}{2Y^2} - \frac{r_z^2}{2Z^2}\right)$	$n_i = n_{i,c} \frac{V_c}{V} \exp\left(-\frac{r_x^2}{2X^2} - \frac{r_y^2}{2Y^2} - \frac{r_z^2}{2Z^2}\right)$
$(1+\kappa)\left[\frac{d}{dT}\frac{\kappa T}{1+\kappa}\right]\frac{\dot{T}}{T} + \frac{\dot{V}}{V} = 0$	$\frac{d(\kappa T)}{dT}\frac{\dot{T}}{T} + \frac{\dot{V}}{V} = 0$
$X\ddot{X} = Y\ddot{Y} = Z\ddot{Z} = \frac{1}{1+\kappa(T)}$	$X\ddot{X} = Y\ddot{Y} = Z\ddot{Z} = \frac{T}{\langle m \rangle}$

Table 2: Parametric solution of fireball hydrodynamics for a tri-axially expanding, non-rotating ellipsoidal fireball, where the volume V and the average mass $\langle m \rangle$ are defined by eqs. (9) and (12). The first two rows give the parametric form of the density and the velocity fields. Note that in these solutions, the corresponding temperature field is homogeneous, $T(t, \mathbf{r}) \equiv T(t)$. The time evolution of the temperature is determined by an ordinary differential equation, that depends on the Equation of State through the function $\kappa \equiv \kappa(T)$ which for a spatially homogeneous temperature field is a function of time only, $\kappa \equiv \kappa(T(t))$. The acceleration of the scales X, Y, Z is driven also by the equation of state, but on the QM side the value of the constant of proportionality, $\frac{1}{1+\kappa(T)}$ is in general different from the value of constant of proportionality in the HM phase, $\frac{T}{\langle m \rangle}$.

QM ($T_i \geq T \geq T_{chem}$)	**HM** ($T_{chem} > T \geq T_f$)
$\mathbf{v} = (\frac{\dot{R}}{R} r_x - \omega r_y, \frac{\dot{R}}{R} r_y + \omega r_x, \frac{\dot{Z}}{Z} r_z)$	$\mathbf{v} = (\frac{\dot{R}}{R} r_x - \omega r_y, \frac{\dot{R}}{R} r_y + \omega r_x, \frac{\dot{Z}}{Z} r_z)$
$\sigma = \sigma_0 \frac{V_0}{V} \exp\left(-\frac{r_x^2}{2R^2} - \frac{r_y^2}{2R^2} - \frac{r_z^2}{2Z^2}\right)$	$n_i = n_{i,c} \frac{V_c}{V} \exp\left(-\frac{r_x^2}{2R^2} - \frac{r_y^2}{2R^2} - \frac{r_z^2}{2Z^2}\right)$
$(1+\kappa)\left[\frac{d}{dT}\frac{\kappa T}{1+\kappa}\right]\frac{\dot{T}}{T} + \frac{\dot{V}}{V} = 0$	$\frac{d(\kappa T)}{dT}\frac{\dot{T}}{T} + \frac{\dot{V}}{V} = 0$
$R\ddot{R} - R^2\omega^2 = Z\ddot{Z} = \frac{1}{1+\kappa(T)}$	$R\ddot{R} - R^2\omega^2 = Z\ddot{Z} = \frac{T}{\langle m \rangle}$

Table 3: Parametric solution of fireball hydrodynamics for a spheroidally expanding, and rotating fireball. Notation is the similar to that of Table 2, but the volume V is defined by eq. (10) and the time evolution of the angular velocity ω is given by eq. (11).

by the radial expansion as follows:

$$\omega(t) = \omega_0 \frac{R_0^2}{R(t)^2}. \tag{11}$$

In this expression ω_0 and R_0 are the initial values of the corresponding functions at the initial time t_0. As the equations of motion for the scales are indepenent from the type of particle i in the HM phase, it is easy to see that the fireball expands collectively to the vacuum, for all particle types i.

Instead of the mass m of a single type of particle in the dynamical equations of a *single component*, chemically frozen HM phase, the average mass $\langle m \rangle$ appears in the dynamics of a *multi-component*, chemically frozen HM phase. The typical value for $\langle m \rangle$ 200 GeV Au+Au collisions at RHIC is given approximately [16] as

$$\langle m \rangle = \frac{\sum\limits_i m_i n_{i,c}}{\sum\limits_i n_{i,c}} \approx 280\ MeV. \tag{12}$$

The same analysis [16] indicated chemical freeze-out temperatures in the range of T_{chem} 150 − 170 MeV. At the chemical freeze-out ($T \approx T_{chem}$), the acceleration changes due to the change of the coefficients that determine $\ddot{X}X$ and similar quantities. To quantify this, we evaluate the right hand side of the acceleration equations at T_{chem}, both in the QM and in the HM phases, using the lattice QCD equation of state, and we find the following relation:

$$\frac{1}{1+\kappa(T_{chem})} \simeq 0.11 - 0.15 < \frac{T_{chem}}{\langle m \rangle} \simeq 0.55 - 0.63. \tag{13}$$

This inequality is thus valid in a broad range of T_{chem}, independently from the actual value of the chemical freeze-out temperature, if this is varied in the reasonable range of $150 < T_{chem} < 175$ MeV [16].

As a consequence, the acceleration of the scales (X, Y, Z) starts to *increase* as the temperature cools just below T_{chem}, for any reasonable value of T_{chem}, not due to the change of the pressure but due to the change of the dynamical equations, that include new conservation laws. This increased acceleration leads to a secondary explosion of the medium, which starts just after the conversion from quark matter to the chemically frozen hadronic matter.

A novel feature of the secondary explosion is that actually this happens at temperatures where the $\kappa = \varepsilon/p$ ratio is close to its maximum in lattice QCD calculations, hence the corresponding speed of sound is nearly minimal. This temperature is usually called the "softest point" of the equation of state, and it is usually associated with a slowing down of the transverse flows, see for example the exact solutions of T. S. Biró for a first order phase transition of a massless gas of quarks and gluons to a massless pion gas [17, 18].

In particular if the pressure could become a constant during a first order phase transition, its gradiends would approach vanishing values, hence the acceleration terms would vanish. However, when we take into account a lattice QCD equation of state, that lacks a first order phase transition at small baryochemical potentials, the pressure gradients do not vanish. Furthermore, at T_{chem}, additional local hadronic conservation laws start to play a role and modify the dynamics. As a consequence of inequality in eq. (13), instead of slowing down, the expansion starts actually to accelerate faster at T_{chem}, as compared to the case when hadronization and hadrochemical freeze-out does not happen!

Another novel and rather surprising feature of this secondary explosion is related to the relative position of the chemical freeze-out to the softest point of the lQCD Equation of State. If the chemical freeze-out temperature T_{chem} is less than $T_{max} \approx 151$ MeV, the temperature where $d\kappa/dT(T = T_{max}) = 0$, this second explosion generated by the hadrochemical freeze-out leads to *faster expansion* as well as *slower cooling*, as compared to an expansion where hadrochemical freeze-out does not happen. This is a rather unusual scenario, as normally faster expansion leads to faster cooling. Such a more usual behaviour is described by the same equations if $T_{chem} > T_{max} = 151$ MeV. As this is the expected range for the chemical freeze-out temperatures [16], we expect that when the secondary, hadrochemical explosion happens, and the fireball starts to expand faster, the cooling of the temperature as a function of time actually becomes also faster.

3 Observables

The observables for a single-component hadronic matter (HM) were already evaluated in refs. [4] and [9]. In this manuscript we present the generalization of these earlier results for the multi-component hadronic matter scenario. The results are summmarized in Tables 4 and 5, corresponding to the solutions in Table 2 and 3, respectively. These results summarize only some of the key, the selected hadronic observables, such as the inverse slope parameters and the HBT-radii. The relation of these key observables to the single particle spectra, elliptic or higher order flows or to the Bose-Einstein correlation functions is the same, as in refs. [6, 9], respectively. In these calculations, the freeze-out temperature is denoted by T_f and subscript f indicates quantities that are evaluated at the time of the kinetic feeze-out.

The inverse slopes and the squared inverse HBT-radii are linear functions of m_i. Recent experimental results of for example the PHENIX collaboration correspond well to these linear relations [19]. As these data were taken in high energy heavy ion collisions, where the hadronic final state contains a mixture of various hadrons (referred to as the multi-component Hadronic Matter scenario), it is a non-trivial result that such simple re-

HM (one kind of hadron only, with mass m)	**HM** (mixture of various hadrons, with masses m_i)
$T_x = T_f + m\dot{X_f}^2$	$T_{x,i} = T_f + m_i\dot{X_f}^2$
$T_y = T_f + m\dot{Y_f}^2$	$T_{y,i} = T_f + m_i\dot{Y_f}^2$
$T_z = T_f + m\dot{Z_f}^2$	$T_{z,i} = T_f + m_i\dot{Z_f}^2$
$R_x^{-2} = X_f^{-2}\left[1 + \frac{m}{T_f}\dot{X}_f^2\right]$	$R_{x,i}^{-2} = X_f^{-2}\left[1 + \frac{m_i}{T_f}\dot{X}_f^2\right]$
$R_y^{-2} = Y_f^{-2}\left[1 + \frac{m}{T_f}\dot{Y}_f^2\right]$	$R_{y,i}^{-2} = Y_f^{-2}\left[1 + \frac{m_i}{T_f}\dot{Y}_f^2\right]$
$R_z^{-2} = Z_f^{-2}\left[1 + \frac{m}{T_f}\dot{Z}_f^2\right]$	$R_{z,i}^{-2} = Z_f^{-2}\left[1 + \frac{m_i}{T_f}\dot{Z}_f^2\right]$

Table 4: Inverse slope parameters for a single component and a multi-component hadronic matter as well as HBT-radii for a triaxially expanding, non-rotating, ellipsoidal fireball, corresponding to the hydrodynamical solution in Table 2. The relation to the single particle spectra and Bose-Einstein correlation functions is the same, as in ref. [6], but instead of the mass m of a single kind of hadron for each hadronic species i their mass m_i appears in the observables.

placement rules: $m \to \langle m \rangle$ in the dynamical equations and $m \to m_i$ in the observables can be utilized to obtain the new exact solutions of the hydrodynamical equations and the evaluation of the obsverables.

4 A new parametrization for lattice QCD EoS

In the earlier sections of this manuscript we presented the transition of a Quark Matter to Hadronic Matter that contained a mixture of various hadrons. These solutions, however, were limited by the assumption of a homogeneous initial temperature profile. In this section we prepare the ground for new solutions where the initial temperature and density profile may be inhomogeneous.

Recently, ref. [8] explored new, exact, parametric solutions of non-relativistic, rotating fireballs, using a lattice QCD equation of state, similarly to our previous studies, but using a single mass m in the hadron gas phase. That work explored two kinds of exact solutions: the first class of solutions had homogeneous temperature profiles, where the local temperature was a function of time only, $T \equiv T(t)$. That class of solutions were generalized to the multi-component hadronic matter in the previous sections of this manuscript. The second class of solutions in ref. [8] allowed for inhomogeneous temperature profiles if the density profiles

HM (single component, with mass m)	**HM** (multi-component, with masses m_i)
$T_x = T_f + m\left(\dot{R}_f{}^2 + \omega_f^2 R_f^2\right)$	$T_{x,i} = T_f + m_i\left(\dot{R}_f{}^2 + \omega_f^2 R_f^2\right)$
$T_y = T_f + m\left(\dot{R}_f{}^2 + \omega_f^2 R_f^2\right)$	$T_{y,i} = T_f + m_i\left(\dot{R}_f{}^2 + \omega_f^2 R_f^2\right)$
$T_z = T_f + m\dot{Z}_f{}^2$	$T_{z,i} = T_f + m_i\dot{Z}_f{}^2$
$R_x^{-2} = R_f^{-2}\left[1 + \frac{m}{T_f}\left(\dot{R}_f^2 + R_f^2\omega_f^2\right)\right]$	$R_{x,i}^{-2} = R_f^{-2}\left[1 + \frac{m_i}{T_f}\left(\dot{R}_f^2 + R_f^2\omega_f^2\right)\right]$
$R_y^{-2} = R_f^{-2}\left[1 + \frac{m}{T_f}\left(\dot{R}_f^2 + R_f^2\omega_f^2\right)\right]$	$R_{y,i}^{-2} = R_f^{-2}\left[1 + \frac{m_i}{T_f}\left(\dot{R}_f^2 + R_f^2\omega_f^2\right)\right]$
$R_z^{-2} = Z_f^{-2}\left[1 + \frac{m}{T_f}\dot{Z}_f^2\right]$	$R_{z,i}^{-2} = Z_f^{-2}\left[1 + \frac{m_i}{T_f}\dot{Z}_f^2\right]$

Table 5: Inverse slope parameters for a single component and a multi-component hadronic matter as well as HBT-radii for a rotating and expanding spheroidal fireball, corresponding to the hydrodynamical solution in Table 3. The relation to the single particle spectra and Bose-Einstein correlation functions is the same, as in ref. [9], but the results for the single component hadron mass are generalized for the multi-component scenario. The new results can be obtained simply, with the help of an $m \to m_i$ replacement .

had a corresponding, matching shape. This second class of solutions was obtained for a special equation of state, where the $\kappa(T) \equiv \kappa_c$ function was a temperature independent constant. We are not interested here in this scenario, as the lattice QCD Equation of State indicates that $\kappa = \varepsilon/p$ is not a temperature independent constant. However, in a footnote of ref. [8], a third class of solutions was also mentioned, noting that solutions exist also for the case of inhomogeneous temperature profiles also in the case of a temperature dependent $\kappa(T)$ functions, if a special differential equation is statisfied by $\kappa(T)$ functions, however, this class was not investigated in detail.

Here we follow up that line of research by demonstrating that the lattice QCD equation of state can be parameterized by $\kappa(T)$ functions that allow for exact solutions of fireball hydrodynamics with inhomogeneous temperature profiles. The criteria to find such hydrodynamical solutions is that the coefficient of the logarithmic comoving derivative of the temperature fields be a constant both in the QM and in the HM phase, as detailed below.

From the temperature equation for high temperatures ($T_i \geq T \geq T_{chem}$), corresponding to the dynamical equations that describe the evolution of QM in Table 1, this criteria leads to the following constraint on the possible shape of the $\kappa(T)$ function:

$$\frac{d}{dT}\left[\frac{T\kappa(T)}{1+\kappa(T)}\right] = \frac{\kappa_Q}{1+\kappa(T)}, \qquad (T \geq T_{chem}), \tag{14}$$

where $\kappa_Q = \lim_{T\to\infty} \kappa(T)$ stands for the high temperature limit of the $\kappa(T)$ function.

As the coefficient of the temperature equation in Table 1 is modified at lower temperatures ($T_{chem} > T > T_f$), corresponding to a multi-component, chemically frozen Hadronic Matter, in this temperature range a modified constraint is obtained for the $\kappa(T)$ function:

$$\frac{d}{dT}\left[T\kappa(T)\right] = \frac{\kappa_c T_c - \kappa_f T_f}{T_c - T_f}. \qquad (T_{chem} > T \geq T_f), \tag{15}$$

where $T_c = T_{chem} = 175\ MeV$ corresponds to the upper limit of the chemical freeze-out temperatures obtained from experimental data on particle ratios in $\sqrt{s_{NN}} = 200$ GeV Au+Au collisions at RHIC [16]. In the above equations, we have assumed that at the kinetic freeze-out the non-relativistic ideal gas approximation can be used i.e. $\kappa_f = \kappa(T_f) = 3/2$, however higher values of κ_f can also be used if one intends to match lattice QCD calculations at lower temperatures closely. In any case, after freeze-out we assume that hadrons propagate to the detectors with free streaming and post kinetic freeze-out their energy density to pressure ratio thus decreases or jumps to the value of $3/2$.

For the QM phase the analytic solution of the constraint (14) is

$$\kappa_{QM}(T) = \frac{\kappa_Q \left(\frac{T}{T_c}\right)^{1+\kappa_Q} + \frac{\kappa_c - \kappa_Q}{\kappa_c + 1}}{\left(\frac{T}{T_c}\right)^{1+\kappa_Q} - \frac{\kappa_c - \kappa_Q}{\kappa_c + 1}}, \tag{16}$$

and in this function κ_c stands for $\kappa(T_c)$. For the HM phase, the solution to the constraint of eq. (15) yields the following form for $\kappa(T)$:

$$\kappa_{HM}(T) = \frac{\kappa_c T_c - \kappa_f T_f}{T_c - T_f} - \frac{\kappa_c - \kappa_f}{T_c - T_f}\frac{T_c T_f}{T}. \tag{17}$$

These solutions are matched at the critical temperature $T_c = 175$ MeV and we have assumed that the chemical freeze-out temperature is the same as the critical temperature, $T_{chem} = T_c$. We made fits to simulated data from lattice QCD [14] using κ_Q as a fitting parameter, for $T_c = 175$ MeV fixed and using various values of the kinetic freeze-out temperature T_f. The quality of these fits is summarized in Table 6 and on Figure 1.

In the QM phase, a satisfactory fit is found, as indicated by the red curve and summarized also in Table 6. We could also obtain reasonably good fits in the HM range of temperatures, however, with some constaints on the possible value of the kinetic freeze-out temperature T_f: A reasonable value of the freeze-out temperature is the pion mass, $T_f \approx 140$ MeV (continuous, blue line) but in this case κ falls down too steeply with temperature due to our additional requirement of $\kappa(T_f) = 3/2$ and it is reflected very well by the unsatisfactory confidence level of this fit. However, fits with freeze-out temperature $T_f \leq 100$ MeV and $\kappa(T_f) = 3/2$ are statistically acceptable.

Curves	χ^2/NDF	CL [%]
lQCD parametrization	0.12/5	> 99.9
$\kappa_Q = 3.833$	6.48/4	16.6
$T_f = 140\ MeV$	86.56/6	$1.6{\cdot}10^{-14}$
$T_f = 100\ MeV$	7.71/6	26.0

Table 6: Confidence levels of parametrizations of the lattice QCD Equation of State, for various values of the freeze-out temperature T_f. Note that in these parameterizations, $\kappa(T_f) = 3/2$, so at freeze-out a non-interacting, ideal gas equation of state is reached.

This section prepares the ground for new exact analytic solutions of hydrodynamics where the initial temperature profile is spatially inhomogeneous. Although such solutions can be obtained by straight-forward generalizations of the exact solutions of ref. [8] with spatially inhomogeneous temperature profiles both in the high temperature QM and in the low temperature HM phases, even for a multi-component hadronic matter scenario, their matching at the chemical freeze-out temperature is an open research question hence these solutions are not detailed here.

5 Conclusions

We described two new classes of exact solutions of fireball hydrodynamics, for a re-hadronizing and expanding fireball, using lattice QCD Equation of State. In the first class of solutions, the expaning ellipsoid is triaxial, but the fireball is not rotating, $(X \neq Y \neq Z, \omega = 0)$. In the second class of solutions, although the expansion is spheroidal, the fireball is rotating, $(X = Y = R \neq Z, \omega \neq 0)$. In both cases, we found that the fireball expands to the vacuum as a whole, although the quark matter rehadronizes to a hadronic matter that includes various hadronic components (for example pions, kaons, protons and all the other measured hadronic species). In both classes of the presented new solutions, the same length and temperature scales characterize the fireball dynamics for all the hadronic types in the final state, $(X \neq X_i, Y \neq Y_i, Z \neq Z_i)$, so the fireball keeps on expanding as a whole, instead of developing non-equilibrium features such as separate lenght-scales for each observable hadrons.

We have obtained a surprising analytic insight to the effects of hadrochemical freeze-out on the expansion dynamics. If rehadronization is immediately followed by a hadrochemical freeze-out, this leads to a modification of the dynamical equations, which in turn leads to a second, violent, hadrochemical explosion. Instead of slowing down the radial flows at the

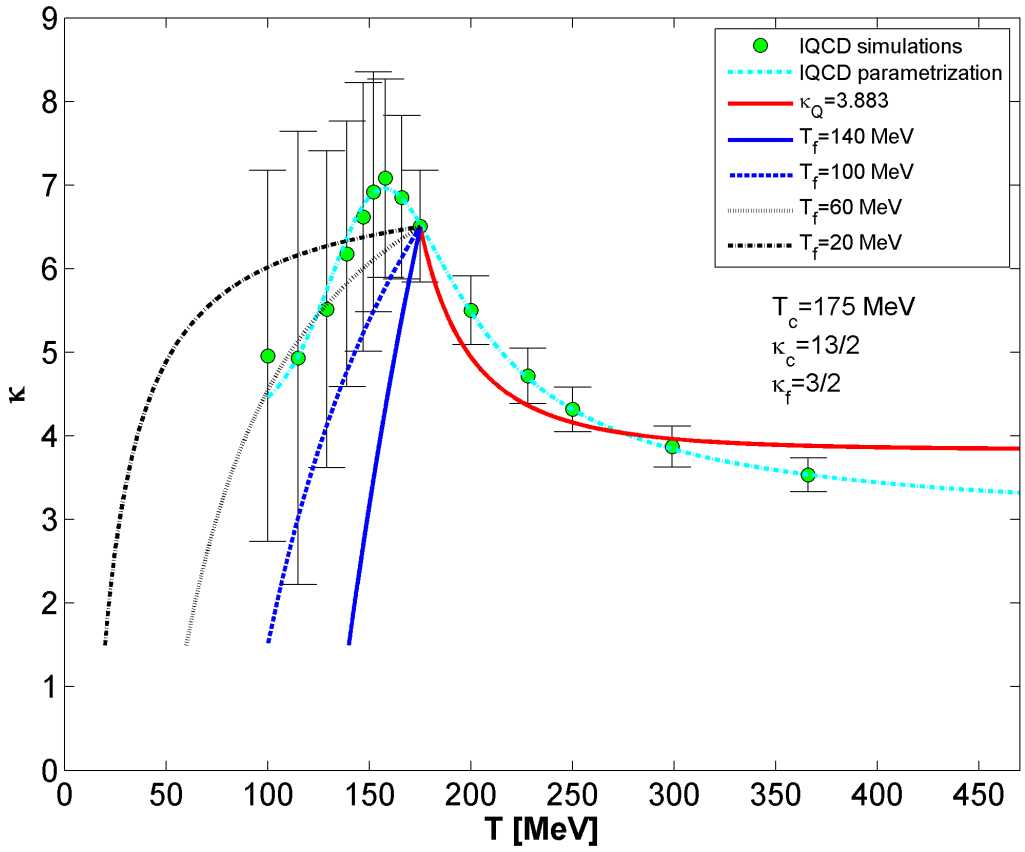


Figure 1: Fits of the hydrodynamically motivated parameterizations above and below T_{chem} to the lattice QCD data points on $\kappa(T) = \varepsilon/p$. In these fits, we required that at freeze-out, a non-relativistic ideal gas limit is approached so that $\kappa(T_f) = 3/2$ and varied the freeze-out temperature from 20 to 140 MeV.

softest point where p/ε is minimal, the expansion dynamics does not slow down, but it actually accelerates. We have found that the expansion dynamics starts to accelerate at the chemical freeze-out temperature due to the inequality (13) which is a consequences of the application of lattice QCD EoS when evaluating the expansion dynamics in Tables 2 and 3. In this hadrochemical explosion, all the length-scales (X, Y, Z) and R start to accelerate faster, when the temperature drops just below $T = T_{chem}$, as compared to a scenario without hadrochemical freeze-out, so in this sense the dynamics becomes “hardest" at the “softest point" of the lattice QCD Equation of State.

In the last section, we have also shown that the lattice QCD equation of state $\kappa(T)$ can be parametrized in a new way, which is suitable for the development of exact and analytic, parametric solutions of fireball hydrodynamics even for an initially inhomogenous temperature profile. The details of this solution with inhomogeneous temperature profile,

as well as the extension of the presented solutions to the relativistic kinematic region are important issues that go beyond the scope of the limitations of this conference contribution.

Acknowledgments

We thank Y. Hatta, D. Klabucar, T. Kunihiro, S. Nagamiya and K. Ozawa for enlightening and useful discussions. T. Cs. would like to thank S. Nagamiya and K. Ozawa for their kind hospitality at KEK, Tsukuba, Japan. This research was supported by the Hungarian OTKA grant NK 101438 as well as by a 2016 KEK Visitor Fund.

References

[1] J. P. Bondorf, S. I. A. Garpman, and J. Zimányi. *Nucl. Phys.*, A296:320–332, 1978.

[2] P. Csizmadia, T. Csörgő, and B. Lukács. *Phys. Lett.*, B443:21–25, 1998.

[3] T. Csörgő. *Central Eur. J. Phys.*, 2:556–565, 2004.

[4] S.V. Akkelin, T. Csörgő, B. Lukács, Yu.M. Sinyukov, and M. Weiner. *Phys. Lett.*, B505:64–70, 2001.

[5] T. Csörgő. *Acta Phys. Polon.*, B37:483–494, 2006.

[6] T. Csörgő, S.V. Akkelin, Y. Hama, B. Lukács, and Yu.M. Sinyukov. *Phys. Rev.*, C67:034904, 2003.

[7] M. I. Nagy, T. Csörgő, and M. Csanád. *Phys. Rev.*, C77:024908, 2008.

[8] T. Csörgő and M.I. Nagy. *Phys.Rev.*, C89(4):044901, 2014.

[9] T. Csörgő, M. I. Nagy, and I. F. Barna. *Phys. Rev.*, C93(2):024916, 2016.

[10] M. I. Nagy and T. Csörgő. `arXiv:1606.0916`, submitted for a publication (2016).

[11] M. Csanád, M. I. Nagy, and S. Lökös. *Eur. Phys. J.*, A48:173, 2012.

[12] I. G. Bearden et al, NA44 Collaboration. *Phys. Rev. Lett.*, 78:2080–2083, 1997.

[13] S. S. Adler et al, PHENIX Collaboration. *Phys. Rev.*, C69:034909, 2004.

[14] Sz. Borsányi, G. Endrődi, Z. Fodor, A. Jakovác, S. D. Katz, et al. *JHEP*, 1011:077, 2010.

[15] S. Z. Belenkij and L. D. Landau. *Nuovo Cim. Suppl.* **3S10**, 15 (1956) [*Usp. Fiz. Nauk* **56**, 309 (1955)].

[16] M. Kaneta and N. Xu, `nucl-th/0405068` .

[17] T. S. Biró, Phys. Lett. B **474**, 21 (2000) [nucl-th/9911004].

[18] T. S. Biró, Phys. Lett. B **487**, 133 (2000) [nucl-th/0003027].

[19] D. Kincses, for the PHENIX Collaboration: *Acta Phys. Polon. Supp.*, 9:243, 2016.